

See discussions, stats, and author profiles for this publication at: <https://www.researchgate.net/publication/262110600>

# Monolayer Assembly of Ferrimagnetic Co<sub>x</sub>Fe<sub>3-x</sub>O<sub>4</sub> Nanocubes for Magnetic Recording

ARTICLE *in* NANO LETTERS · MAY 2014

Impact Factor: 13.59 · DOI: 10.1021/nl500904a · Source: PubMed

---

CITATIONS

11

---

READS

71

## 8 AUTHORS, INCLUDING:



Liheng Wu

Brown University

13 PUBLICATIONS 767 CITATIONS

[SEE PROFILE](#)



Alshakim Nelson

IBM

57 PUBLICATIONS 1,724 CITATIONS

[SEE PROFILE](#)



Huiyuan Zhu

Brown University

20 PUBLICATIONS 367 CITATIONS

[SEE PROFILE](#)



Sen Zhang

University of Pennsylvania

28 PUBLICATIONS 1,093 CITATIONS

[SEE PROFILE](#)

# Monolayer Assembly of Ferrimagnetic $\text{Co}_x\text{Fe}_{3-x}\text{O}_4$ Nanocubes for Magnetic Recording

Liheng Wu,<sup>†</sup> Pierre-Olivier Jubert,<sup>‡</sup> David Berman,<sup>‡</sup> Wayne Imaiño,<sup>‡</sup> Alshakim Nelson,<sup>‡</sup> Huiyuan Zhu,<sup>†</sup> Sen Zhang,<sup>†</sup> and Shouheng Sun<sup>\*,†</sup>

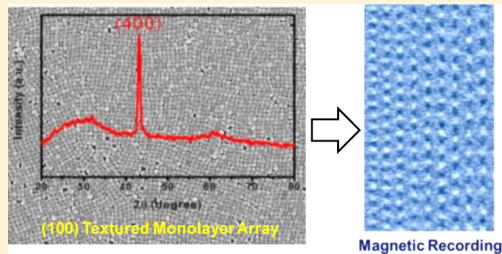
<sup>†</sup>Department of Chemistry, Brown University, Providence, Rhode Island 02912, United States

<sup>‡</sup>IBM Almaden Research Center, 650 Harry Road, San Jose, California 95120, United States

## Supporting Information

**ABSTRACT:** We report a facile synthesis of monodisperse ferrimagnetic  $\text{Co}_x\text{Fe}_{3-x}\text{O}_4$  nanocubes (NCs) through thermal decomposition of  $\text{Fe}(\text{acac})_3$  and  $\text{Co}(\text{acac})_2$  ( $\text{acac}$  = acetylacetone) in the presence of oleic acid and sodium oleate. The sizes of the NCs are tuned from 10 to 60 nm, and their composition is optimized at  $x = 0.6$  to show strong ferrimagnetism with the 20 nm  $\text{Co}_{0.6}\text{Fe}_{2.4}\text{O}_4$  NCs showing a room temperature  $H_c$  of 1930 Oe. The ferrimagnetic NCs are self-assembled at the water–air interface into a large-area (in square centimeter) monolayer array with a high packing density and (100) texture. The 20 nm NC array can be recorded at linear densities ranging from 254 to 31 kfci (thousand flux changes per inch). The work demonstrates the great potential of solution-phase synthesis and self-assembly of magnetic array for magnetic recording applications.

**KEYWORDS:** Cobalt ferrite, nanocube, ferrimagnetic, self-assembly, data storage



The need for long-term and cost-effective digital archives requires state-of-the-art magnetic tape products with ever-increased areal storage density.<sup>1–4</sup> To support such a high recording density, magnets used for tape recording must be made in the nanometer-size regime and assembled with both their packing density maximized and their magnetization direction oriented. Conventional nanomagnets developed as magnetic tape media have been based on ferrimagnetic (FIM) iron oxides in needle-like shapes due to their acceptable shape-induced anisotropy/coercivity, medium high magnetization, high Curie temperature, and more importantly, their excellent chemical stability and corrosion resistance. Once stabilized with oxide coating, rod-shaped FeCo alloy particles have been used in tape media products, enabling recording densities up to 2 Gb/in<sup>2</sup>. Recently, the demand for even higher recording density requires the nanomagnets to be smaller and smaller, and shape anisotropy cannot be used to support such a dimension reduction. Ferrite magnets with a large magnetocrystalline anisotropy, such as cobalt ferrite ( $\text{CoFe}_2\text{O}_4$  or  $\text{CoO}\cdot\text{Fe}_2\text{O}_3$ )<sup>5</sup> and hexagonal barium hexaferrite ( $\text{BaFe}_3$ ,  $\text{BaO}\cdot 6\text{Fe}_2\text{O}_3$ , or  $\text{BaFe}_{12}\text{O}_{19}$ ),<sup>6</sup> have been considered as alternative media materials. For example, doped  $\text{BaFe}_{12}\text{O}_{19}$ , which are now used in commercial tape drives, have led to a 29.5 Gb/in<sup>2</sup> recording demonstration.<sup>7</sup> Magnetic studies have shown that magnetocrystalline anisotropy constant ( $K$ ) of the nonstoichiometric Co-substituted magnetite  $\text{Co}_x\text{Fe}_{3-x}\text{O}_4$  and hexagonal BaFe can be as high as  $5 \times 10^5 \text{ J/m}^3$ ,<sup>8,9</sup> which are close to those of the common hard magnetic FePt, SmCo, and NdFeB magnets at  $10^6$ – $10^7 \text{ J/m}^3$ .<sup>10,11</sup> These suggest that  $\text{Co}_x\text{Fe}_{3-x}\text{O}_4$  or BaFe, once prepared in a proper nanometer size and shape,

can maintain large magnetic coercivity, providing a more cost-effective system than other noble metal (FePt) and rare-earth metal (SmCo and NdFeB) magnets for magnetic tape applications.

Herein we report a new approach to FIM Co-ferrite nanocubes (NCs) and monolayer assemblies and demonstrate their capability for magnetic recording. Previously we developed a high-temperature solution phase synthesis of monodisperse  $\text{CoFe}_2\text{O}_4$  nanoparticles (NPs) via thermal decomposition of  $\text{Fe}(\text{acac})_3$  and  $\text{Co}(\text{acac})_2$  ( $\text{acac}$  = acetylacetone) in the presence of oleic acid and oleylamine.<sup>12</sup> We extended this synthesis and prepared monodisperse  $\text{Co}_x\text{Fe}_{3-x}\text{O}_4$  NPs with  $x$  tuned by the molar ratio of  $\text{Co}(\text{acac})_2/\text{Fe}(\text{acac})_3$ .<sup>13</sup> These FIM NPs were dispersible in hexane, and random assemblies had coercivities reaching as high as 3.1 kOe at room temperature. However, the size of these Co-ferrite NPs was around 35 nm, which was too large for high-density recording. We further improved the synthesis by replacing oleylamine with sodium oleate and found that FIM Co-ferrite nanocubes (NCs) were produced with their sizes (10–20 nm) and composition ( $\text{Co}_{0.6}\text{Fe}_{2.4}\text{O}_4$ ) controlled by the  $\text{Co}(\text{acac})_2/\text{Fe}(\text{acac})_3$  ratio. More importantly, these FIM NCs were well-dispersed in hexane, allowing for self-assembly. We developed an organic liquid–water phase self-assembly approach and succeeded in depositing monolayer assembly of these FIM

**Received:** March 10, 2014

**Revised:** May 5, 2014

**Published:** May 6, 2014

NCs on a solid substrate. These monolayer arrays showed FIM at room temperature and could be recorded using a static magnetic tester. The work demonstrates the great potential of Co-ferrite NCs as promising alternative media for tape recording applications.

The  $\text{Co}_x\text{Fe}_{3-x}\text{O}_4$  NCs were synthesized by the thermal decomposition of  $\text{Fe}(\text{acac})_3$  and  $\text{Co}(\text{acac})_2$  in benzyl ether at 290 °C for 1 h. Oleic acid and sodium oleate were used as surfactants to direct the anisotropic growth. The as-synthesized NCs were characterized by transmission electron microscopy (TEM). Figure 1A shows the typical TEM image of the as-

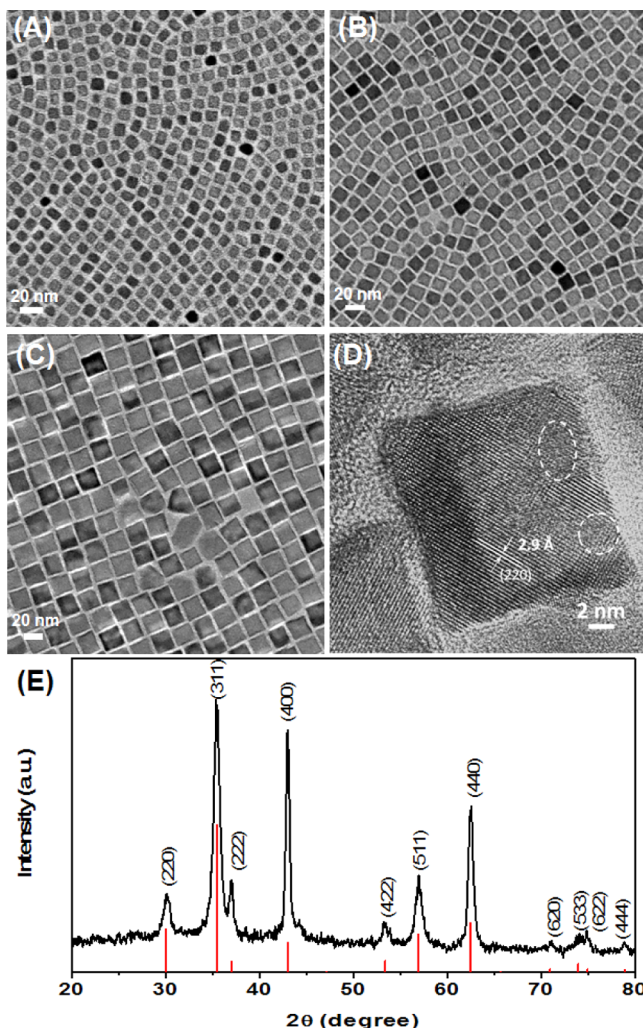


**Figure 1.** TEM images of the as-synthesized (A) 10 nm, (B) 15 nm, and (C) 20 nm  $\text{Co}_{0.6}\text{Fe}_{2.4}\text{O}_4$  NCs; (D) HRTEM image of a single 20 nm NC; (E) XRD pattern of the powder dried from hexane dispersion of 20 nm NCs.

synthesized NPs deposited on an amorphous carbon-coated Cu grid. These NCs have an average edge size of  $10 \pm 0.7$  nm. By increasing the amount of  $\text{Fe}(\text{acac})_3$  and  $\text{Co}(\text{acac})_2$  while keeping other parameters unchanged, larger NCs were synthesized. Figure 1B and C shows the TEM images of larger NCs with the size of  $15 \pm 0.6$  nm and  $20 \pm 1$  nm, respectively. The Co compositions in those NCs were determined by using inductively coupled plasma–atomic emission spectroscopy (ICP-AES). All of the three kinds of NCs showed the same composition of  $\text{Co}_{0.6}\text{Fe}_{2.4}\text{O}_4$ , which was in the right range for

optimized magnetic coercivity.<sup>8</sup> The 20 nm NCs were further characterized by high-resolution TEM (HRTEM) (Figure 1D), which shows lattice fringes with the interfringe distance in a single NC at 2.9 Å, close to the lattice spacing of (220) planes at 2.96 Å in the reverse spinel  $\text{CoFe}_2\text{O}_4$ . Also the diagonal direction of (220) planes further confirmed the cubic shape of the nanoparticle. Some crystal defects were found in the HRTEM image as marked by dashed ellipses. These defects were probably caused by O vacancies formed in the inert reaction atmosphere. Figure 1E is the X-ray diffraction (XRD) pattern of the 20 nm NC powder dried from the hexane dispersion. The diffraction pattern corresponds well with the inverse spinel crystal structure of  $\text{CoFe}_2\text{O}_4$ , which shows clear (220), (311), (222), (400), (422), (511), and (440) diffraction peaks.

To better understand the role of the surfactants in the NC growth, we did some control experiments. For the synthesis of 20 nm  $\text{Co}_{0.6}\text{Fe}_{2.4}\text{O}_4$  NCs showing in Figure 1C, 350 mg of  $\text{Fe}(\text{acac})_3$  reacted with 140 mg of  $\text{Co}(\text{acac})_2$  in the presence of 300 mg of sodium oleate and 2 mL of oleic acid. Without sodium oleate, polyhedral NPs were synthesized (Supporting Information, Figure S1A). This indicates that the formation of NCs was initiated by the preferred binding of sodium oleate to the {100} planes, which promoted the faster growth along ⟨111⟩ directions. Oleic acid in the synthesis not only acts as the surfactant but also as the growth rate controller. For example, larger NCs (60 nm) were synthesized by decreasing the amount of oleic acid to 1.5 mL while maintaining other reaction conditions (Figure S1B). It is worth emphasizing that enough precursors are also critical for the formation of cubic NPs. By just decreasing the amount of cobalt precursors from 140 to 120 mg, smaller (15 nm) polyhedral NPs rather than NCs were obtained, as shown in Figure S1C. It seems that, due to the lack of enough monomers, the growth along ⟨111⟩ direction was not complete, which resulted in truncated cubic NPs. ICP analysis showed that the composition of the NPs was  $\text{Co}_{0.4}\text{Fe}_{2.6}\text{O}_4$ , which had lower Co content compared to the 20 nm NCs. However, if the amount of cobalt precursors was increased to 160 mg, the {111} were fully developed, and NCs were formed. Then more precursors resulted in larger NCs (25 nm) as confirmed by TEM image in Figure S1D. The composition was determined to be  $\text{Co}_{0.7}\text{Fe}_{2.3}\text{O}_4$ , which was more Co-rich than the 20 nm NCs. Our synthesis indicates that both surfactants and precursors need to be controlled in a proper amount to achieve the anisotropic growth of the Co-ferrite NPs into cubic shape and controlled compositions.

Magnetic properties of the  $\text{Co}_{0.6}\text{Fe}_{2.4}\text{O}_4$  NCs were characterized by a vibrating sample magnetometer (VSM) with fields up to 14.5 kOe at room temperature. The hysteresis loops of the as-synthesized NCs are shown in Figure 2A. These NCs exhibited clear size-dependent magnetic properties. For the 10 nm NCs, the coercivity was just 15 Oe. As the size increased to 15 nm, the coercivity increased to 170 Oe correspondingly. Further increasing the size to 20 nm resulted in the enhancement of coercivity to 810 Oe. Considering the defects present in each NP (Figure 1D) may result in low magnetic anisotropy of the ferrite NPs, we annealed the ferrite NPs in  $\text{O}_2$  at 300 °C for 1 h. Figure 2B shows the hysteresis loops of the NCs after the annealing. The coercivity of the 10 nm, 15 nm, and 20 nm NCs were significantly increased to 550 Oe, 1200 Oe, and 1930 Oe, respectively. Besides, the saturation moment ( $M_s$ ) of the NCs also increased after the annealing treatment. For instance, the  $M_s$  of 20 nm NCs enhanced to 78

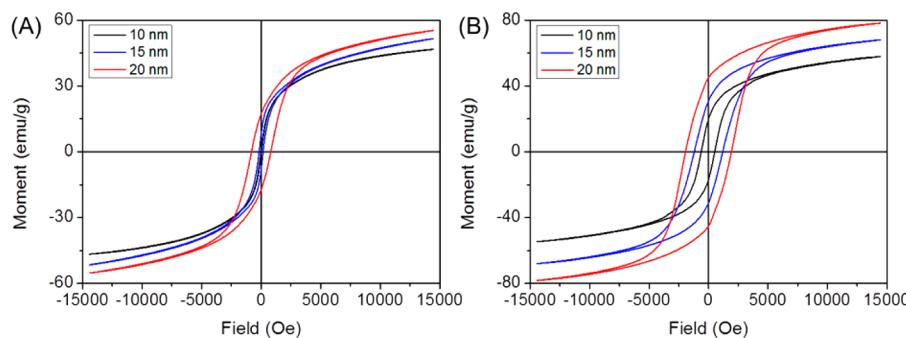


**Figure 2.** Hysteresis loops of (A) the as-synthesized NCs without annealing and (B) the NCs after annealing in oxygen at 300 °C for 1 h.

emu/g, which was much higher than that of as-synthesized ones (55 emu/g). The TEM image of the 20 nm NCs after annealing shows no aggregation/sintering (Figure S2A). The HRTEM image of a single NC after annealing is shown in Figure S2B, which clearly exhibits perfect lattice fringes of (400) planes in the single crystalline NC. The control experiment of annealing the NCs in inert Ar gas at 300 °C for 1 h shows that there is no obvious magnetic property change between the annealed and the as-synthesized NCs (Figure S3). The controlled annealing and its effect on magnetic properties confirm that the defects observed in the as-synthesized ferrite NC (Figure 1D) indeed lead to decreased coercivity and annealing under O<sub>2</sub> is necessary to remove these defects and to increase magnetic anisotropy.

To test the potential of these FIM NCs for data storage applications, they must first be assembled in uniform arrays with a high packing density. We utilize the self-assembly technique at the liquid–air interface to fabricate ordered monolayer NC arrays for magnetic recording demonstration.<sup>14,15</sup> We improved the liquid–air interfacial assembly and developed a facile approach to assemble NCs at organic solvent and water interface. To make the monolayer assembly, 120 μL of the NCs dispersion in the mixture of toluene and hexane (volume ratio 1:1) with the concentration of 0.5 mg/mL was drop-cast on the water surface in a Teflon column (diameter, 3.8 cm) and then dried at room temperature. By using the mixture of toluene and hexane, the evaporating rate was slowed which favored the NC face-to-face interaction for the assembly formation. After complete evaporation of the toluene and hexane, the monolayer film formed on the water surface was transferred onto Cu TEM grids or Si substrates for further characterization. Figure 3A shows the TEM image of the self-assembled monolayer array of the 20 nm Co<sub>0.6</sub>Fe<sub>2.4</sub>O<sub>4</sub> NCs. Scanning electron microscopy (SEM) image of the self-assembled NCs is shown in Figure 3B, which further confirms the formation of large-area densely packed monolayer. The crystal orientation of each NC in the self-assembly was further characterized by X-ray diffraction (XRD) (Figure 3C). Different from the randomly oriented powder diffraction pattern of the 20 nm NCs which shows a strong (311) diffraction peak in Figure 1E, the XRD pattern of the self-assembled monolayer on Si substrate exhibits only one (400) diffraction peak. This (400)-only diffraction further indicates that NCs in the monolayer assembly have a preferred orientation along the <100> direction. Similar large-area monolayer films of 15 and 10 nm NCs were also obtained (Figure S4) by using the water–air interfacial self-assembly.

We chose the monolayer assembly of the 20 nm Co<sub>0.6</sub>Fe<sub>2.4</sub>O<sub>4</sub> NCs deposited on a Si substrate to demonstrate their capability

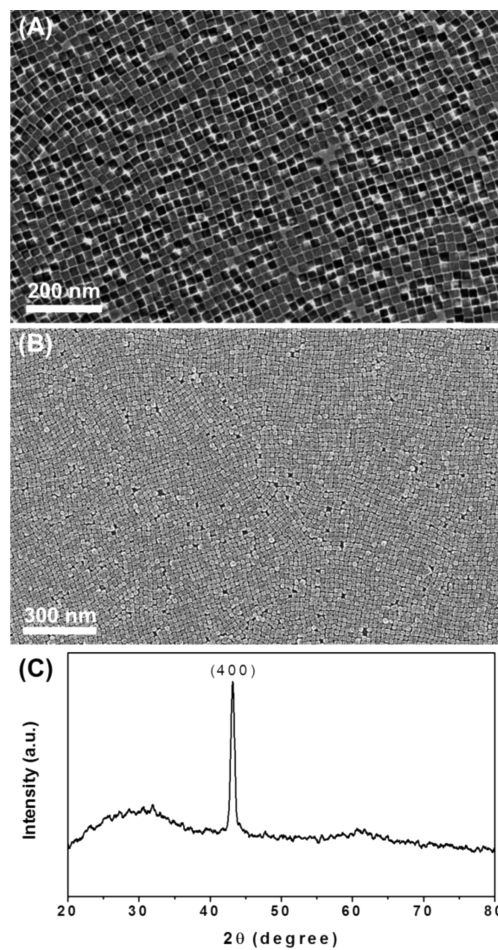


**Figure 3.** Self-assembled monolayer of the 20 nm NCs. (A) TEM image, (B) SEM image, and (C) XRD pattern of the monolayer assembly deposited on a Si substrate.

in recording magnetization transitions. To ensure the assembly was magnetically and mechanically robust for the recording demonstration, we first annealed the monolayer assembly at 300 °C in O<sub>2</sub> for 1 h. Figure 4A shows the SEM image of the annealed monolayer assembly. After this post-treatment the monolayer array was well-maintained without any aggregation or sintering. Magnetic properties of the monolayer assembly were measured using VSM at room temperature. Due to the very weak signal of the monolayer, hysteresis loops were obtained roughly by subtracting the background signal from Si. As shown in Figure S5, O<sub>2</sub> annealing indeed increased the coercivity of the NCs in monolayer assembly. The monolayer

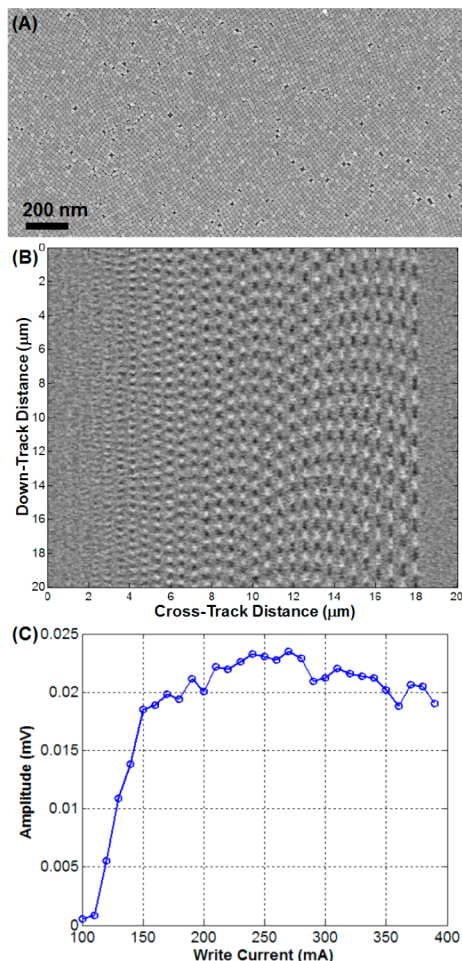


**Figure 4.** (A) SEM image of the monolayer film after annealing at 300 °C for 1 h in oxygen. (B) Magnetic field image of the readback amplitude at linear densities ranging from 254 to 31 kfci. (C) Dependence of signal amplitude on the write current.

assembly was further coated with a 15 nm SiN film deposited via sputtering step to protect the NC layer from scratching by the magnetic recording head. The magnetic recording characteristics of the monolayer assembly were measured using a contact magnetic tester. The monolayer array was first written by the writing head with different linear densities that reflect the number of magnetization reversal changes per unit length. The recorded information was sensed by a read head in the form of voltage. Figure 4B is the magnetic field image of the readback amplitude at linear densities ranging from 254 to 31 kfci (thousand flux change per inch) with the “black” and “white” blocks representing reversal magnetization directions. The tracks are written along the vertical direction. The leftmost track corresponds to the highest linear density of 254 kfci. The linear density in the subsequent tracks toward the right is decreased with the rightmost track, corresponding to the lowest linear density of 31 kfci. The signal amplitude increased while decreasing the linear densities of the writing signal. At the linear bit density of 125 kfci, the signal exhibited a sufficiently strong signal to enable the study of the dependence of signal amplitude on write current, which is shown in Figure 4C. The signal amplitude enhanced while increasing the write current from 100 mA but saturated at around 250 mA. To further assess the write/read performance of the monolayer assembly, the signal-to-noise ratio (SNR) of the readback signal

was tested at different linear bit densities, as shown in Figure S6. It can be found that the SNR value was around 10 dB at linear densities below 200 kfci, indicating that the signal could be easily resolved above the noise. Thus, these write/read experiments clearly demonstrate that the monolayer assembly of the ferrimagnetic  $\text{Co}_{0.6}\text{Fe}_{2.4}\text{O}_4$  NCs can indeed be used as a magnetic recording medium.

In conclusion, we have reported an improved and facile approach to ferrimagnetic ferrite NCs of  $\text{Co}_x\text{Fe}_{3-x}\text{O}_4$ . The NCs are synthesized by high-temperature decomposition of  $\text{Fe}(\text{acac})_3$  and  $\text{Co}(\text{acac})_2$ , and the NC shapes are controlled by oleic acid and sodium oleate. The synthesis allows easy control of NC sizes (from 10 to 60 nm) and Co/Fe compositions, and  $\text{Co}_{0.6}\text{Fe}_{2.4}\text{O}_4$  NCs are found to be optimal to show ferrimagnetism with the 20 nm NCs having a room temperature  $H_c = 1930$  Oe. The well-dispersed ferrimagnetic NCs can be assembled into monolayer array at the water–air interface, and the monolayer array in centimeter square is readily transferred onto a solid substrate. The NCs in the monolayer array are densely packed and (100) textured. Once annealed in air and coated with a thin (15 nm) SiN film, the NC array becomes robust and can be used to record magnetic patterns. Our magnetic writing experiments show that the 20 nm NC monolayer array can be recorded at linear densities ranging from 254 to 31 kfci (thousand flux change per inch), indicating the potential of self-assembled monolayer array as magnetic recording media. Our synthesis and self-assembly methods are not limited to ferrite NCs but can be extended to other functional nanoparticles as well, providing a unique approach to monolayer nanoparticle array for important technological applications.

## ■ ASSOCIATED CONTENT

### S Supporting Information

Experimental section and Figures S1–S6. This material is available free of charge via Internet at <http://pubs.acs.org>.

## ■ AUTHOR INFORMATION

### Corresponding Author

\*E-mail: ssun@brown.edu.

### Notes

The authors declare no competing financial interest.

## ■ ACKNOWLEDGMENTS

This work was supported by the Information Storage Industry Consortium (INSIC).

## ■ REFERENCES

- (1) Dee, R. H. *MRS Bull.* **2006**, *31*, 404–408.
- (2) Argumedo, A. J.; Berman, D.; Biskeborn, R. G.; Cherubini, G.; Cideciyan, R. D.; Eleftheriou, E.; Haberle, W.; Hellman, D. J.; Hutchins, R.; Imaiño, W.; Jelitto, J.; Judd, K.; Jubert, P. O.; Lantz, M. A.; McClelland, G. M.; Mittelholzer, T.; Narayan, C.; Olcer, S.; Seger, P. J. *IBM J. Res. Dev.* **2008**, *52*, 513–527.
- (3) Holzner, F.; Paul, P.; Drechsler, U.; Despont, M.; Knoll, A. W.; Duerig, U. *Appl. Phys. Lett.* **2011**, *99*, 023110.
- (4) Fontana, R. E.; Hetzler, S. R.; Decad, G. *IEEE Trans. Magn.* **2012**, *48*, 1692–1696.
- (5) Dai, Q.; Berman, D.; Virwani, K.; Frommer, J.; Jubert, P. O.; Lam, M.; Topuria, T.; Imaiño, W.; Nelson, A. *Nano Lett.* **2010**, *10*, 3216–3221.
- (6) Kolev, S.; Lisjak, D.; Drofenik, M. *J. Exp. Nanosci.* **2011**, *6*, 362–373.

- (7) Cherubini, G.; Cideciyan, R. D.; Dellmann, L.; Eleftheriou, E.; Haeblerle, W.; Jelitto, J.; Kartik, V.; Lantz, M. A.; Olcer, S.; Pantazi, A.; Rothuizen, H. E.; Berman, D.; Imaino, W.; Jubert, P. O.; McClelland, G.; Koeppe, P. V.; Tsuruta, K.; Harasawa, T.; Murata, Y.; Musha, A.; Noguchi, H.; Ohtsu, H.; Shimizu, O.; Suzuki, R. *IEEE Trans. Magn.* **2011**, *47*, 137–147.
- (8) Nlebedim, I. C.; Snyder, J. E.; Moses, A. J.; Jiles, D. C. *IEEE Trans. Magn.* **2012**, *48*, 3084–3087.
- (9) Golubenko, Z. V.; Ol'khovik, L. P.; Popkov, Y. A.; Sizova, Z. I.; Kamzin, A. S. *Phys. Solid State* **1998**, *40*, 1718–1720.
- (10) Weller, D.; Moser, A. *IEEE Trans. Magn.* **1999**, *35*, 4423–4439.
- (11) Weller, D.; Doerner, M. F. *Annu. Rev. Mater. Sci.* **2000**, *30*, 611–644.
- (12) Sun, S. H.; Zeng, H.; Robinson, D. B.; Raoux, S.; Rice, P. M.; Wang, S. X.; Li, G. X. *J. Am. Chem. Soc.* **2004**, *126*, 273–279.
- (13) Yu, Y. S.; Mendoza-Garcia, A.; Ning, B.; Sun, S. H. *Adv. Mater.* **2013**, *25*, 3090–3094.
- (14) Dong, A. G.; Chen, J.; Vora, P. M.; Kikkawa, J. M.; Murray, C. B. *Nature* **2010**, *466*, 474–477.
- (15) Wen, T.; Majetich, S. A. *ACS Nano* **2011**, *5*, 8868–8876.